Title

A Time- and Compartment-Specific Activation of Lung Macrophages in Hypoxic Pulmonary Hypertension

Journal

The Journal of Immunology, 198(12)

ISSN

0022-1767

Authors

Pugliese, Steven C
Kumar, Sushil
Janssen, William J
et al.

Publication Date

2017-06-15

DOI

10.4049/jimmunol.1601692

Peer reviewed

HHS Public Access

Author manuscript

J Immunol. Author manuscript; available in PMC 2018 June 15.

Published in final edited form as:

J Immunol. 2017 June 15; 198(12): 4802–4812. doi:10.4049/jimmunol.1601692.

A Time and Compartment Specific Activation of Lung Macrophages in Hypoxic Pulmonary Hypertension[1]

Steven C Pugliese[1,5], **Sushil Kumar**[1], **William J Janssen**[2,5], **Brian B Graham**[5], **Maria G Frid**[1], **Suzette R Riddle**[1], **Karim C. El Kasmi**[4], and **Kurt R. Stenmark**[1]

[1]Cardiovascular Pulmonary Research Laboratories, Departments of Pediatrics and Medicine, University of Colorado Anschutz Medical Campus, Denver, CO

[2]Department of Medicine, National Jewish Health, Denver, CO

[3]Division of Allergy and Immunology, Department of Medicine, University of Colorado School of Medicine, Denver, Colorado

[4]Department of Pediatrics, Division of Gastroenterology, Hepatology, and Nutrition, University Colorado Denver, CO

[5]Division of Pulmonary Sciences and Critical Care Medicine, Department of Medicine, University of Colorado School of Medicine, Denver, Colorado

Abstract

Studies in various animal models suggest an important role for pulmonary macrophages in the pathogenesis of pulmonary hypertension (PH). Yet, the molecular mechanisms characterizing the functional macrophage phenotype relative to time and pulmonary localization/ compartmentalization remain largely unknown. Here, we utilized a hypoxic murine model of PH in combination with flow cytometry assisted cell sorting (FACS) to quantify and isolate lung macrophages from two compartments over time and characterized their programing via RNA sequencing (RNAseq) approaches. In response to hypoxia, we found an early increase in macrophage number that was restricted to the interstitial/perivascular compartment, without recruitment of macrophages to the alveolar compartment or changes in the number of resident alveolar macrophages. Principle component analysis demonstrated significant differences in overall gene expression between alveolar (AMs) and interstitial macrophages (IMs) at baseline and after 4 and 14 days hypoxic exposure. AM's at both day 4 and 14 and IM's at day 4 shared a conserved "hypoxia program" characterized by mitochondrial dysfunction, pro-inflammatory gene activation and mTORC1 signaling, while IM's at day 14 demonstrated a unique anti-

[1]This work was supported by National Institutes of Health Grants: 1R01HL114887-03 (K.R.S); 5 P01 HL014985-40A1(K.R.S.). The Flow Cytometry and the Genomics and Microarray Shared Resources receive support from the National Institutes of Health/National Cancer Institute (University of Colorado Cancer Center Support Grant P30 CA046934).

Correspondence to: Karim C. El Kasmi; Kurt R. Stenmark.

Disclosures:
The authors have no financial conflicts of interest

Public Database deposition:
The RNA-seq data presented in this article have been submitted to the National Center for Biotechnology Information Gene Expression Omnibus repository (http://www.ncbi.nlm.nih.gov/geo/). Data will be immediately available up publication. Accession number GEO Submission (GSE87602

inflammatory/ pro-reparative programming state. We conclude that the pathogenesis of vascular remodeling in hypoxic PH involves an early compartment independent activation of lung macrophages towards a conserved hypoxia program, with the development of compartment specific programs later on in the course of disease. Thus, harnessing time and compartment specific differences in lung macrophage polarization needs to be considered in the therapeutic targeting of macrophages in hypoxic PH and potentially other inflammatory lung diseases. (word count 243)

Keywords

Macrophage; pulmonary hypertension; mTOR; hypoxia; polarization; inflammation; remodeling

Introduction

Monocyte/macrophage accumulation within the perivascular/adventitial space is a consistent feature of pulmonary vascular remodeling associated with pulmonary hypertension (PH), both in humans and in all animal models(1). In patients with pulmonary arterial hypertension (PAH), adventitial macrophages remain the most prominent inflammatory cell type within the vessel wall even in those with end stage disease undergoing lung transplantation (2). Studies in various animal models have demonstrated a critical role for perivascular macrophages in the vascular remodeling process associated with PH (3–5). While less known about the role of the alveolar macrophage (AM) in hypoxic PH, they are able to directly affect cells/tissues outside of the alveolar space and in their absence, hypoxic PH is attenuated (6–8). Yet, the stimuli that promote macrophage recruitment and activation remain ill defined. We have recently reported in humans and animal models of PH that adventitial fibroblasts are able to recruit, retain, and activate macrophages, at least in part through paracrine IL6, resulting in activation of STAT3 and HIF1 signaling and prominent expression of pro-remodeling genes, including Arginase 1 (*Arg 1*) (9). Similarly, Vergadi et al demonstrated in a hypoxic mouse model of PH that alveolar macrophages are polarized towards a slightly different phenotype, also characterized by increased expression of *Arg1* (10). Overexpression of heme-oxygenase 1 reduced expression of these genes in alveolar macrophages and attenuated hypoxic PH (10). Together these data are in support of the hypothesis that macrophages with a pro-remodeling phenotype play a critical role in vascular remodeling associated with PH. However, the functional macrophage phenotype in terms of cellular pathways suited to promote the initiation and perpetuation of vascular remodeling and how these pathways differ relative to onset of hypoxia exposure and lung compartment (alveolar versus interstitial/perivascular) have not been determined.

Increased knowledge regarding compartment and time specific pulmonary macrophage activation phenotypes could aid in the design of therapeutics to attenuate pulmonary vascular remodeling. A major barrier to better define macrophage phenotypes within the lung has been difficulty in isolating macrophages from interstitial and perivascular lung compartments. As a consequence, recent studies have solely focused on characterizing alveolar macrophages or have relied on using in vitro approaches which fall short of adequately recapitulating the in vivo microenvironment. Here we utilized flow cytometric

approaches in combination with RNA sequencing (RNAseq) in a hypoxic mouse model of PH to isolate macrophages from the alveolar and interstitial/perivascular compartments at different time points to interrogate macrophage polarization relative to time and compartment. A time course experiment demonstrated that macrophage recruitment occurred early (day 4 hypoxic exposure) and was restricted to the interstitial/perivascular compartment, without recruitment of macrophages to the alveolar compartment or changes in the number of resident alveolar macrophages. Our RNAseq data suggest that the pathogenesis of vascular remodeling in hypoxic PH involves an early compartment independent activation of lung macrophages towards a conserved hypoxia program, while later on in the course of disease macrophages diverge to reveal unique compartment specific programs. The implication of this finding is that the development of therapeutic targets for PH needs to consider this temporo-spatial aspect of macrophage activation.

Methods

Animals

Eight week old C57B6 male mice born at Jackson Labs (Jackson Laboratories, Maine, USA) were kept at simulated sea level altitude for one week after arrival with controlled temperature (22–24 °C) under a 12-hour-light– dark cycle. Food and water were accessible ad libitum. After 1 week at sea level, mice were placed in hypobaric hypoxic chambers for a time course of simulated hypoxia at 18,000 feet as previously described (11). Control mice (normoxia) were kept at sea level altitude under the same light–dark cycle. Standard veterinary care was according to institutional guidelines in compliance with Institutional Animal Care and Use Committee–approved protocols.

Immunostaining

Frozen O.C.T.-embedded 5um cryosections from control mice (n = 5) and mice exposed to hypoxia for 4- and 14 days (n=5/group) were processed for indirect immunofluorescent analysis as previously described(11). Briefly, sections were fixed in cold Acetone:Methanol (1:1); incubated with primary rat monoclonal antibody against macrophage marker CD68 (1:300 dilution, AbD Serotec (Raleigh, NC)), and detection was performed via a Biotin-Streptavidin system using Alexa-594 fluorochrome according to manufacturer's manual (Molecular Probes/Invitrogen, Frederick, MD). Stained sections were mounted with VectaShield embedding medium with DAPI (Vector Labs, Burlingame, CA), and examined under a Zeiss fluorescent microscope. Images were acquired using AxioVision digital imaging system.

Tissue preparation and flow cytometry

Bronchoalveolar fluid was obtained after 4 serial lavages with 1ml PBS with 2mm EDTA. Cells were washed, pelleted and resuspended in staining buffer, PBS with 1% Hyclone FBS (GE healthcare life sciences). An aliquot was removed, stained with trypan blue, and counted via hemocytometer. For lung tissue, mice were anesthetized with inhaled isoflurane and injected retroorbitally with 4ul of CD 45 antibody (clone 30-F11, BD biosciences). After 5 minutes, mice were sacrificed and lung tissues perfused with PBS and minced.

Lungs were digested with collagenase A (40units/ml) (Roche) and DNase I (10,000 units/ml) (Thermoscientific) for 30 min at 37C, pelleted at 350 × g, lysed with RBC lysis buffer (Ebiosciences) for 5 min at RT, washed and filtered through a 70uM nylon mesh filter, and resuspended in PBS with staining buffer. Prior to staining, FcγR was blocked with anti-CD16/CD32 Ab (BD Biosciences) for 10 min. Cells were stained for 30–45 min at 4ºC with a combination of the following antibodies: CD45-APC-Cy7 (clone 30-F11, BD biosciences), CD64-AF647 (clone X54-5/7.1, BD Biosciences), CD11b-BV510 (clone M1/70, BD Biosciences), CD11c-FITC (clone HL3, BD Biosciences) Ly6G-EF450 (clone 1A8, BD Biosciences), CD3-V450 (clone17A2, BD Biosciences), CD45R-V450 (clone RA3-6B2, BD Biosciences). Prior to flow cytometry, cells were filtered through a 40um filter, washed, pelleted and resuspended in staining buffer or sorting buffer (PBS, 1mM EDTA, 25mM HEPES pH 7.0, 1% FBS). Flow cytometry analysis and cell sorting were conducted at the University of Colorado Cancer Center Flow Cytometry Core Facility using a Gallios 561 flow cytometer (Beckman Coulter) for analysis and XDP-100 (Beckman Coulter) cell sorters for sorting. FACS counting beads (BD biosciences) were used to calculated absolute cell numbers during analysis. The sorting strategy involved exclusion of debris and cell doublets by light scatter and dead cells by DAPI (1 mg/ml). Cells were sorted into 1mL Hanks Balanced Salt Solution (Thermofisher) with 1% Hyclone FBS. Purity checks were performed on all samples. Data were analyzed using Kaluza software (Beckman Coulter) and FloJo software (FlowJo).

RNA extraction, qPCR and RNA-seq

For RNA isolation and subsequent RNA-seq, cells were pooled from 3 mouse lungs and performed in biologic triplicate. Total RNA was isolated from flow cytometry cells using a hybrid of Trizol (Ambion) extraction and Qiagen RNeasy MinElute clean up kit (Qiagen). Cells were lysed in Trizol, Chloroform was added in a 1:5 ratio, pelleted at 12,000xg for 15 minutes, aqueous layer removed and combined 1:1 with 100% ethanol, and placed into Qiagen MinElute column. RNA was further cleaned up per RNeasy MinElute protocol (Qiagen). RNA quality and quantity were analyzed using a NanoDrop and Bioanalyzer. First-strand cDNA synthesis was performed using an iScript cDNA Synthesis Kit (Bio-Rad, Hercules, CA). Quantitative RT-PCR was performed using TaqMan probes and reagents (Applied Biosystems, Grand Island, NY), according to the manufacturer’s instructions. Gene expression was calculated after normalization to Hprt1 using the D/D Ct method. RNA-seq library preparation and sequencing were conducted at the Genomics and Microarray Core at the University of Colorado Denver–Anschutz Medical Campus. Libraries were constructed using a NuGen Ovation human FFPE RNA-seq multiplex system kit customized with mouse specific oligonucleotides for rRNA removal. Directional mRNA-seq was conducted using the Illumina HiSeq 2000 system, using the single-read 100 cycles option.

Bioinformatics

Derived sequences were analyzed by applying a custom computational pipeline consisting of the open-source gSNAP, Cufflinks, and R for sequence alignment and ascertainment of differential gene expression (CITES) (11, 12). In short, reads generated were mapped to the mouse genome (mm10) by gSNAP, expression (FPKM) derived by Cufflinks, and

differential expression analyzed with ANOVA in R. Data were analyzed through the use of QIAGEN's " Ingenuity Pathway Analysis " (IPA) (QIAGEN Redwood City, www.qiagen.com/ingenuity). By using RNA pooled from 3 mice and performing experiments in biologic triplicate (except AM sea level performed in biologic replicate) we had a power of 99% for sample size and a p value of <0.05 in all macrophage populations. IPA analysis was performed on a filtered dataset for each of the macrophage sets with the cutoff values of: q <0.05, absolute 2 fold change from baseline, FKPM >5 in any one comparison. The corresponding sea level macrophage was used as a baseline for comparison, ie sea level alveolar macrophage compared to hypoxic day 4 alveolar macrophage.

Results

During hypoxia exposure lung macrophage recruitment is restricted to the perivascular space

We first wanted to determine if macrophage numbers in the alveolar and interstitial compartments change over time in response to hypoxia. Using a qualitative histologic approach, we confirmed that in response to hypoxia exposure, CD68 macrophages accumulate early (day 4) in the perivascular space with a waning in perivascular macrophages by day 14 (Fig 1). We did not observe increased staining for CD68 in the alveolar compartment in hypoxic mice relative to normoxic mice (Fig 1). To more definitively quantify resident and recruited macrophages within the alveolar and interstitial compartments over time, we next utilized a flow cytometry approach. C57B6J mice were exposed to 4, 7, 14, or 28 days of hypobaric hypoxia (18,000ft) or sea level (SL) and at day of sacrifice, lung tissue was enzymatically digested and macrophages were analyzed using flow cytometry. To isolate distinct macrophage populations, we utilized a flow cytometry technique in which lung macrophages and monocytes are separated into 3 compartments: the alveolar compartment by identifying CD64+, CD11c^{hi}, CD11b^{lo}, intravenous (IV)-CD45- cells, the interstitial compartment by identifying CD64+, CD11c^{lo}, CD11b^{hi}, IV-CD45−, and the intravascular or marginated compartment by identifying CD64dim, CD11b^{hi}, IV-CD45+ cells (Suppl Fig 1) (13). By injecting mice with intravenous CD45 antibody (Ab) 5 minutes before euthanasia, marginated leukocytes (IV CD45 Ab^{+} cells) that are unable to be flushed from the vasculature can be excluded(13). The remaining IV Ab CD45^{-} lung parenchymal cells, after exclusion of dead cells, T and B lymphocytes, and neutrophils, were defined as macrophages by CD64 expression and then further separated into alveolar and non-alveolar macrophages based on expression of CD11c and CD11b: alveolar CD11c ^{hi}, CD11b^{lo} and non-alveolar CD11c ^{lo}, CD11b^{hi}. While these cells are leukocytes and therefore express CD45, they do not stain for IV injected CD45 antibody (13). Because of the difficulty in resolving the interstitial space from the perivascular or peribronchoalveolar spaces by microscopy due to the often overlapping spatial arrangement, along with the inability to differentiate macrophages based on cell surface markers in these sometimes separate compartments we collectively refer to macrophages in these spaces as interstitial macrophages (IM's) and will refer to them as CD11b^{hi} macrophages. Conversely, we will refer to the AM's as CD11c^{hi} macrophages. Using the above mentioned FACS strategy, we observed that during the analyzed time course there was an accumulation of CD11b^{hi} IM's

which was maximal after 4 days of hypoxia and decreased thereafter to baseline levels by day 14, further supporting our histologic analysis in figure 1 (Fig 2a, Suppl Fig 1b). A semiquantitative approach demonstrated that the percentage of IM's was increased at day 4 and returned to near baseline around day 14 (Suppl Fig 1b). This finding further was confirmed using a quantitative FACS counting bead approach (Fig 2a). While there was a reciprocal decrease in AM's after 4 days of hypoxia using a semiquantiative approach (Suppl Fig 1c), there were no changes in AM number when quantified using highly accurate FACS counting beads (Fig 2b, Suppl Fig 1d). Furthermore, there were no differences in AM's in bronchoalveolar lavage (BAL) fluid quantified by counting beads or hemocytometer (Fig 2c). Importantly, we did not detect $CD11b^{hi}$ positive cells in the alveolar space at any time point which further confirms the absence of macrophage recruitment to the alveolar space (Fig 2d) and explains why the number of alveolar macrophages did not change. Therefore, $CD11c^{hi}$ positive macrophages were restricted to the alveolar space and $CD11b^{hi}$ positive macrophages appeared to be recruited to and remain within the interstitial space.

Alveolar and interstitial macrophage programming is unique at baseline and in response to hypoxia exposure

We next employed RNAseq analysis to obtain an unbiased and comprehensive display of gene expression profiles and signaling pathways in alveolar and interstitial macrophage subsets at baseline and in response to hypoxia. Based on the results obtained in the time course analysis depicted above (Fig 2), we chose to perform RNAseq on day 0 (i.e. mice that remained at sea level), and on day 4 and 14 of hypoxic exposure. We utilized the FACS sorting strategy described in Figure S1a because it most clearly defines macrophages in the alveolar and interstitial compartment and carefully excludes any cells in the intravascular compartment (Suppl Fig 1a). Principle component analysis (PCA) validated previous observations that naïve $CD11c^{hi}$ AM's and $CD11b^{hi}$ IM's are very different at baseline (14) (Fig 3a). In response to hypoxia, IM's and AM's significantly alter their gene expression, and continue to remain significantly different from one another through 14 days hypoxia. (Fig 3a). Interestingly, the PC1, which separates the IM's from the AM's was determined to be 20%, while the PC2, which separates sea level from hypoxia exposure, was determined to be 17%, suggesting that the differences that separate sea level from hypoxic macrophages are nearly as great as those that separate AM's from IM's (Fig 3a).

Lung macrophages demonstrate both unique and shared programs in response to hypoxia

While the overall gene expression of these macrophage subsets are significantly different at baseline and in response to hypoxia, we wanted to determine if there are any shared "hypoxic programs" in the two macrophage populations over time. We hypothesized that due to compartment specific differences in the microenvironment, AM's and IM's would demonstrate unique programming changes in response to hypoxia over time. For identification of differentially expressed genes in the RNAseq data between the cell populations (IM & AM) and between different time points (sea level, 4 & 14 days hypoxia) we used the following cutoff criteria: fragments per kilobase of exon per million fragments mapped (FKPM) ≥ 5 in at least one condition and have ≥ 2 fold change in any comparison with a false discovery rate- adjusted p value, $q<0.05$. In all pairwise comparisons we

identified 2,672 statistically significant differentially expressed genes based on above criteria and we used these set of genes for pathway analysis and functional annotations study. We generated a global heatmap displaying all 2,672 differentially expressed genes between the various macrophage subsets (Fig 3b). The heatmap demonstrates several important findings: 1. Hypoxia significantly altered gene expression in both IM's and AM's. 2. Both shared and unique gene expression profiles in IM's and AM's in response to hypoxia were observed. 3. Gene expression profiles in AM's at day 4 and 14 are virtually indistinguishable, while there was significant heterogeneity between IM's at day 4 and 14. AM's shared about 2/3 of differentially expressed genes between day 4 and 14, while less than half of those were shared in IM's between day 4 and 14, further suggesting that AM's have a more conserved gene expression response to hypoxia relative to IM's (Fig 4). The VENN diagrams also highlight that in AM's there is an increasing number of up regulated genes through day 14, while IM's exhibit maximal up regulation of genes at day 4, which decline by day 14 (Fig 4). Combined with data shown in the heatmap, this suggests that IM's undergo a polarization shift with an attenuation in overall gene expression between day 4 and 14.

Hypoxia leads to early compartment independent activation of lung macrophages towards a conserved hypoxia program and later to compartment specific programs

Ingenuity pathway analysis (IPA) was used to interrogate the major pathways and specifically compare the programming changes within the two macrophage subsets (IM's and AM's) over time. IPA was performed utilizing the 2,762 differentially expressed genes from the heatmap (fig 3b) (q value <0.05, fold change ≥ 2 fold). This software is able to organize genes into known pathways with p value as a reflection of the percentage of genes in the database that are in the pathway, and z score which predicts whether the pathway is activated or inhibited. We used the highly significant cutoffs of: p value <0.05 and absolute Z score ≥ 2. In AM's, the top canonical pathways and upstream regulators were largely the same at day 4 and 14 with a trend toward increasing polarization at day 14, as reflected by increasing Z scores in nearly all pathways (increasingly more negative or more positive) between days 4 and 14 (Fig 5a,b). Conversely, in IM's, nearly all of the top canonical pathways and upstream regulators observed to be increased at day 4 were decreased by day 14 (Fig 5a,b). This is reflected by an absolute reduction in Z score (less negative or positive) in those pathways at day 14 (Fig 5a,b). Additionally, we found that the most differentially expressed pathways and upstream regulators were largely the same in AM's throughout the hypoxic time course and in IM's at day 4, but not in day 14 IM's (Fig 5a,b). These findings are also evident when AM's from both time points are directly compared to day 4 IM's (Suppl Fig 2a) and to day 14 IM's (Suppl Fig 2b). Taken together these pathway analyses suggest that, early on, lung macrophages in both compartments are polarized towards a common hypoxic response program. Later in the course of hypoxic exposure, AMs continue to maintain this activation state while IMs become generally less inflammatory and in fact express anti-inflammatory genes (see below). Importantly, many canonical pathways and upstream regulators in day 14 IM's are inhibited relative to baseline macrophages.

In response to hypoxia, alveolar macrophages and early interstitial macrophages are characterized by increased mTORC1 signaling and changes in metabolism

Because the gene expression changes in AM's at days 4 and 14 are very similar to those seen in IM's at day 4, we grouped these three subsets together in an effort to determine the major pathways that define the postulated "hypoxia program". To do this we created data tables with all the major canonical pathways (Fig 5a) and upstream regulators with an absolute Z score cutoff of 2 and a p value <0.05 (suppl table I). Additionally, we created a canonical pathways table using a p value cutoff of < 0.05 in case there were highly significant pathways in which a Z score could not be calculated (Fig 5c). The top general canonical pathways shared between the 3 subsets included increased EIF2, Rho A, and actin cytoskeleton signaling as well as changes in cell metabolism including oxidative phosphorylation, mitochondrial dysfunction, and glycolysis (Fig 5a,b,c). Additionally, cholesterol biosynthesis was highly significant as well, but this appeared to be unique to alveolar macrophages (Fig 5c). Further inspection of the common canonical pathways and upstream regulators revealed a much more specific "hypoxia program" that is defined by activation of innate immune pathways that converge on increased mTORC1 signaling (suppl table I, Fig 5a, Fig 6). Specific upstream regulators included inhibition of RICTOR/mTORC2 and MAP4K4 and activation of EIF2-AK2, ERK, EIF4, mTORC1, MYC, FOXO1 and ERK all consistent with mTORC1 activation, and inhibition of mTORC2 (suppl table I). The major innate immune upstream regulators included activation of HIF1, IFNG, IL1B, NFKB, STAT3, MYD88, TNF, and TLR (suppl table I). Figure 6 summarizes the intersection between mTORC1, metabolism and innate immunity. To further elucidate the individual genes that characterize this cohort of macrophages, we created a table of all the differentially expressed genes (q value <0.05, fold change ≥ 2 fold) that are shared within the cohort of AM's at days 4 and 14 and IM's day 4, but not differentially expressed in IM's at D14 (suppl table II). AM's at days 4 and 14 along with IM's at day 4 share upregulation of a host of specific genes implicated in the pathway analysis above: pro-inflammatory/remodeling genes: Mif, S100a4, Thbs1, Il1b, Ccl4. Metabolism: Pkm, Pgk1, Ldha. MTOR signaling: Lamtor1, 5, Eif4e. FKPM values between samples were remarkably consistent between the biologic samples and further validate this data (Suppl Fig 2c).

After 14 days of hypoxia, interstitial macrophages re-program to anti-inflammatory and pro-reparative/pro-remodeling signaling

As demonstrated in Figures 5a,b, there was a considerable similarity between major canonical pathways and upstream regulators in IM's at days 4 and 14 when compared to sea level controls. However, we wanted to determine which programming changes were unique to day 14 IM's. As shown in figure 7a, the only major canonical pathway with an absolute Z score ≥ 2 ($p < 0.05$) that was different in IM's at day 14 was "Role of pattern recognition receptors in bacteria and viruses" which was down-regulated in IM day 14 ($Z = -2.24$) and unchanged in IM's at day 4. Similarly, we identified the top upstream regulators with an absolute Z score ≥ 2 that were different from IM's at day 4 (Fig 7b). As indicated in figure 7b, most of the up-regulated pathways are anti-inflammatory, while down-regulated pathways are pro-inflammatory. Consistent with these findings, when we analyzed the specific genes that are uniquely differentially expressed in IM day 14 compared to the cohort of AM's at days 4 and 14 and IM's at day 4, we found downregulation of a host of pro-

inflammatory genes including Il6, Mapkapk2, Ccl2, Irf7, Fgfr1 and Thbs1 (Supp table II). FKPM values were similar among biologic replicate samples further validating this data (Suppl Fig 2c). To further validate these findings, we performed qPCR using a few genes from the RNAseq dataset that have been implicated in hypoxic pulmonary hypertension. We show that the qPCR data (normalized to HPRT and Day 4 hypoxia) is largely in line with the RNAseq data for the corresponding genes (Suppl Fig 2d). The error bars are large and do not meet statistical significance due to fairly significant changes in HPRT in response to hypoxia and inter-sample variability (mean of 3 samples). In our experience, there is no ideal housekeeping gene for hypoxia exposure and RNAseq data is much less variable and does not rely on normalization to housekeeping genes.

Next, to more specifically address the programming changes that occur only between 4 and 14 days hypoxia, we used day 4 IM's as a baseline and compared that to day 14 IM's (All prior comparisons used sea level macrophages as baseline). Because the differences were subtle, we used a cuff-off criteria of q value of <0.2 and fold change of ≥1.5 to maximize the number of pathways (Suppl table I). Again, we found changes in programming that predicted activation of anti-inflammatory and pro-remodeling/reparative pathways and inhibition of those that are pro-inflammatory (Fig 8). Therefore, between 4 and 14 days of hypoxia, there exists a programming shift in interstitial macrophages to a phenotype that expresses anti-inflammatory and pro-reparative genes and pathways. Interestingly, this programming change occurs concomitantly with a marked reduction in the number of perivascular macrophages and not only represents an attenuated phenotype from IM's at day 4, but a completely unique phenotype as compared to a naïve resident IM

Discussion

The specific effects of hypoxia on cells which reside within the lungs and its subsequent role in the development of pulmonary vascular remodeling and pulmonary hypertension is well described (15). Additionally numerous groups have demonstrated the importance of monocytes and macrophages in the development of hypoxic pulmonary hypertension (3–5, 10). Due to the inherent difficulties in identifying and isolating lung macrophages in vivo, no one has attempted to carefully phenotype the programs which characterize macrophages in humans or any animal model of pulmonary hypertension. Using the hypoxic mouse model of pulmonary hypertension and a combination of flow cytometry and RNA sequencing approaches, we present for the first time a detailed characterization of gene expression profiles and signaling pathways in alveolar and interstitial/perivascular macrophages over the time course of hypoxic exposure. We found that initially in response to hypoxia, lung macrophages in both alveolar and interstitial compartments display a conserved "hypoxia program" characterized by mitochondrial dysfunction, pro-inflammatory gene activation and mTORC1 signaling, while later in the course of hypoxia interstitial macrophages re-program to a unique anti-inflammatory/pro-reparative state. While others have compared programming of naïve AM's and IM's under resting conditions, ours is one of the first reports to directly compare the two in a disease state (14, 16). To maximize the validity of our bioinformatics data, RNAseq was performed on samples in biologic triplicate with 3 pooled mice per sample utilizing stringent cutoff criteria for our bioinformatics. While we relied on IPA pathway analysis for much of the data analysis, we went a step further to

confirm the major differentially expressed genes among the various macrophage cohorts agreed with the bioinformatics approach and further demonstrate the consistency of FKPM values among multiple genes within the biologic samples.

Consistent with our previous observation in hypoxic rats, we found that hypoxia leads to the early accumulation of macrophages to the interstitial/perivascular space (3). While, our flow cytometry techniques cannot distinguish whether the increase in $CD11b^{hi}$ interstitial macrophages comprises interstitial, perivascular, or peri-bronchoalveolar macrophages, our complimentary histological findings argue in favor of these macrophages being mostly perivascular. Our findings are in line with and further extend previous observations by Amsellem et al who also reported no change in total lung macrophages but increased F4/80+ perivascular macrophages after 18 days of hypoxia in mice (4). Although we did not perform lineage tracing experiments, the increased numbers of perivascular macrophages are likely due to the recruitment of circulating cells and not local proliferation (3, 17). An unexpected and important finding of our study was that we did not observe accumulation of recruited $CD11b^{hi}$ macrophages in the alveolar space nor did we find increases in the numbers of resident CD11c alveolar macrophages throughout the time course of hypoxia. Thus our study challenges a current hypothesis that the increased numbers of alveolar macrophages are due to recruitment of circulating cells (10, 18). This hypothesis was mainly based upon the finding that the monocyte recruitment chemokine MCP-1 was reported to be increased in whole lung tissue and secreted by alveolar macrophages into the alveolar space and systemic circulation in response to hypoxia, although the latter may not be true in mice (8, 19, 20). Increased numbers of BAL macrophages reported by others and observed within hours of hypoxia exposure in rats likely represents increased inflammation-induced lavagability, as the time point chosen in these studies is too early to explain recruitment of macrophages to the alveolar space or cell division to occur (21, 22). Other groups demonstrating increased numbers of alveolar macrophages in response to hypoxia quantified alveolar macrophages only in BAL fluid at slightly different time points, but not whole lung (4, 10). Because only a small percentage of alveolar macrophages are lavagable (fig 2b, c), we quantified AM's in whole lung tissue and BAL using FACS counting beads which provide the most accurate methodology available (23, 24). Therefore, our data support that alveolar macrophages consist of a single population of resident cells which remain quantitatively steady throughout the time course of hypoxia. Conversely, the interstitial macrophages consist of a single population of resident cells at baseline, a mixed population of resident and recruited cells after 4 days of hypoxia, and a more homogenous population of re-programmed macrophages with some recruited cells after 14 days of hypoxia.

We made the somewhat expected observation that alveolar and interstitial macrophages demonstrate significantly different gene expression profiles at baseline and after hypoxia exposure, likely due to differences in microenvironments and ontogeny (25). Intriguingly, despite the large overall differences in gene expression between IM's and AM's, we found that after 4 days hypoxia exposure, there were a large number of shared gene expression profiles between the two, suggesting an early common response pattern to hypoxia. This finding is surprising given that the microenvironments of the alveolar and interstitial spaces during hypoxia exposure demonstrate important differences with regard to oxygen tension, changes in shear stress/blood flow and cell-cell interactions, such that one would expect

compartment specific responses. Moreover, IM's are a mixed population of resident and recruited cells at this time point. This gene expression program was characterized by activation of genes involved in mTORC1 signaling, metabolism and innate immunity. We propose that if it were technically feasible to sort resident from recruited IM's at day 4, further gene expression differences between the two would be discernable (17). As the hypoxic time course progresses, the AM's continue to exhibit a polarized phenotype similar to that observed at day 4, while the IM's undergo a programming shift. As the number of IM's is reduced between day 4 and 14, we found an expected down-regulation of the inflammatory pathways that were increased at day 4. Intriguingly, this IM population at day 14 displayed a transcriptional profile characterized by activation of anti-inflammatory and pro-reparative pathways and inactivation of those that are pro-inflammatory. More importantly, this polarization state of the hypoxic IM's at day 14 was different from that observed in sea level resident macrophages and was characterized by expression of various anti-inflammatory genes, indicating a distinct anti-inflammatory phenotype. When compared to a naïve resident IM at sea level, this distinct macrophage shows inhibition of a host of pro-inflammatory pathways including toll-like receptor (TLR), extracellular signal-regulated kinase (ERK), interferon signaling with activation of the anti-inflammatory pathway including dual specificity phosphatase-1 (DUSP1), heme oxygenase 1 (HMOX-1), Serine/threonine kinase 11 (STK11), and liver x receptors (LXR). MAP kinase phosphatase-1 (MPK-1), also known as DUSP1, appears to be important in limiting the inflammatory response and arginase expression in hypoxic PH, as its deletion leads to exaggerated PH and arginase I/II expression in whole mouse lung (26). Consistent with this, arginase 1 is 108 fold increased in IM's at day 4 compared to sea level, while only 22 fold increased by day 14 (data not shown). Additionally, DUSP1 has been shown to be crucial to limiting LPS induced inflammatory responses in macrophages (27). Hmox1 overexpression attenuates hypoxic PH and appears to mediate the protective effects of rapamycin, the MTOR inhibitor, on hypoxic PH (10, 20, 28). STK11 phosphorylates and activates 5′ adenosine monophosphate-activated protein kinase (AMPK) leading to a host of anti-inflammatory effects including down-regulation of mTORC1 and HIF1a (29). While little is known regarding LXR's in PH, macrophage specific LXR signaling is important in inhibiting macrophage activation and is anti-fibrotic via inhibition of macrophage recruitment and macrophage-induced IL6 release (30–33). While hypoxic mice demonstrate only mild pulmonary vascular remodeling, we found that connective tissue grown factor (CTGF), a well-established mediator of pulmonary vascular remodeling in PH, was activated in day 14 IM's relative to day 4 IM's (34, 35). We hypothesize that the coordinated "anti-inflammatory" and "pro-reparative" programming state in IM's in hypoxic mice limits progressive perivascular remodeling seen in other animal models of PH.

The hypoxic mouse model of PH is characterized by early mild inflammation and pulmonary vascular remodeling with a marked reduction in whole lung inflammation by day 14 onwards and complete resolution of remodeling upon return to normoxia (20, 36). Considering this, we speculate that the day 14 IM polarization state might play an important role in regulating lung inflammation in response to hypoxia and even act to suppress chronic non-resolving inflammation and vascular remodeling. Future studies will have to be designed to examine this hypothesis perhaps by selectively depleting IMs at different time

points during hypoxic exposure. Intriguingly, a similar anti-inflammatory and pro-resolving macrophage phenotype has been found in other fibrosis models, where deletion of macrophages during the fibrotic phase attenuated fibrosis, while deletion of macrophages during the later reparative phase promoted fibrosis (37). Nearly identical findings were reported in a bleomycin lung fibrosis mouse model as well (38). Furthermore, in humans with diabetic foot ulcers, isolation of pro-inflammatory macrophages predicted non-healing ulcers while wounds containing anti-inflammatory macrophages were more likely to undergo wound healing (39). Therefore, we hypothesize that in severe forms of hypoxic PH characterized by persistent pulmonary vascular remodeling, including monocrotaline rats, neonatal calves and some humans, the polarization of the perivascular macrophage fails to shift towards an anti-inflammatory phenotype akin to the one described here (3, 15, 40, 41).

The hypoxic program that characterized alveolar macrophages and early (day 4) interstitial macrophages included changes in mTORC1 signaling, metabolism and activation of innate immune pathways, all well described with regard to hypoxia and pulmonary hypertension (42–45). While the role of innate immune pathways including NFKB, IL1B, IL6, toll like receptor signaling, interferon gamma, HIF-1, and STAT3 signaling are well described with regard to their roles in pulmonary hypertension, very little is known within the context of macrophages in PH (9, 46–54). We previously demonstrated that ex-vivo fibroblasts isolated from neonatal calves and humans with PH polarize macrophages via paracrine IL-6 to a phenotype characterized by increased expression of STAT3, HIF1, and Arginase 1(9). mTORC1 signaling is increased in the lungs and specifically in pulmonary artery smooth muscle cells from animal models and humans with PH and its inhibition attenuates experimental PH (42, 43, 55, 56). mTOR signaling appears to be crucial for macrophage polarization with LPS activated macrophages (M1) displaying an mTORC1/glycolytic phenotype while IL4 activated macrophages (M2) demonstrate increased mTORC2 expression and fatty acid oxidation(57). In dendritic cells, this TLR induced glycolytic shift was found to be HIF1a dependent and induced by nitric oxide and type 1 interferon production (44). Additionally mTORC1 activation in macrophages has been closely linked with IL1B and NLRP3 inflammasome activation in response to LPS (58). While an M1/M2 paradigm is to simplistic to describe in vivo macrophage programming, our data support the idea that hypoxic AM’s and early IM’s appear to be skewed towards an M1-like program with an integrated network of signaling consistent with that described in the context of hypoxia and pulmonary hypertension (59).

The implication of our finding is that the development of therapeutic targets for PH needs to consider a temporo-spatial aspect of macrophage activation as there appears to be potentially opposing roles of macrophages in the development of hypoxic PH. A better understanding of this may facilitate attempts to harness reparative macrophage functions or re-program inflammatory macrophages in the lung to attenuate vascular remodeling. This work represents only a scratching of the surface at understanding the precise role of macrophages in hypoxic PH as important basic questions remain to be answered. For instance, the recruitment of circulating monocytes to the perivascular space appears to be necessary for the development of hypoxic PH, however the relative contributions from interstitial and alveolar macrophages in both the initiation and maintenance of pulmonary vascular remodeling remain unknown (3). To sort out the relative contribution of AM’s and IM’s in

hypoxic PH, we would have to employ transgenic mice in which macrophages can be cleanly and efficiently deleted only in the alveolar or interstitial compartments, however, these mice currently do not exist (60). Despite this, recent evidence suggests we may be able to distinguish resident from recruited arterial macrophages based on cell surface markers(17). Combining very efficient macrophage deletion systems, ie hCD68-rtTA-tetDTA (diptheria toxin mediated CD68 macrophage deletion) with the various known cell surface markers that distinguish macrophage subsets should allow for the creation of transgenic mice that can answer these questions and many more in any mouse lung injury model(61, 62).

Supplementary Material

Refer to Web version on PubMed Central for supplementary material.

Acknowledgments

We thank the members of the University of Colorado Cancer Center Flow Cytometry Core for assistance with flow cytometry and the Genomics and Microarray Core for assistance with RNA-seq. We would like to thank Peter Henson PhD, DVM for his assistance with the manuscript and guidance with experiments and Alex Mckeon for her assistance with immunostaining. Lastly, we would like to thank Dr. Kenneth Jones PhD for his expertise with RNAseq analysis.

References

1. Stenmark KR, Yeager ME, El Kasmi KC, Nozik-Grayck E, Gerasimovskaya EV, Li M, Riddle SR, Frid MG. The Adventitia: Essential Regulator of Vascular Wall Structure and Function. Annu Rev Physiol. 2013; 75:23–47. [PubMed: 23216413]
2. Savai R, Pullamsetti SS, Kolbe J, Bieniek E, Voswinckel R, Fink L, Scheed A, Ritter C, Dahal BK, Vater A, Klussmann S, Ghofrani HA, Weissmann N, Klepetko W, Banat GA, Seeger W, Grimminger F, Schermuly RT. Immune and Inflammatory Cell Involvement in the Pathology of Idiopathic Pulmonary Arterial Hypertension. Am J Respir Crit Care Med. 2012; 186:897–908. [PubMed: 22955318]
3. Frid MG, Brunetti JA, Burke DL, Carpenter TC, Davie NJ, Reeves JT, Roedersheimer MT, Van Rooijen N, Stenmark KR. Hypoxia-Induced Pulmonary Vascular Remodeling Requires Recruitment of Circulating Mesenchymal Precursors of a Monocyte/Macrophage Lineage. The American Journal of Pathology. 2006; 168:659–669. [PubMed: 16436679]
4. Amsellem V, Lipskaia L, Abid S, Poupel L, Houssaini A, Quarck R, Marcos E, Mouraret N, Parpaleix A, Bobe R, Gary-Bobo G, Saker M, Dubois-Randé JL, Gladwin MT, Norris KA, Delcroix M, Combadière C, Adnot S. CCR5 as a treatment target in pulmonary arterial hypertension. Circulation. 2014; 130:880–891. [PubMed: 24993099]
5. Sartina E, Suguihara C, Ramchandran S, Nwajei P, Rodriguez M, Torres E, Hehre D, Devia C, Walters MJ, Penfold MET, Young KC. Antagonism of CXCR7 attenuates chronic hypoxia–induced pulmonary hypertension. Pediatr Res. 2012; 71:682–688. [PubMed: 22337226]
6. Chao J, Wood JG, Gonzalez NC. Alveolar macrophages initiate the systemic microvascular inflammatory response to alveolar hypoxia. Respiratory Physiology & Neurobiology. 2011; 178:439–448. [PubMed: 21402178]
7. Nagai H, Kuwahira I, Schwenke DO, Tsuchimochi H, Nara A, Ogura S, Sonobe T, Inagaki T, Fujii Y, Yamaguchi R, Wingenfeld L, Umetani K, Shimosawa T, Yoshida K-I, Uemura K, Pearson JT, Shirai M. Pulmonary Macrophages Attenuate Hypoxic Pulmonary Vasoconstriction via β3AR/iNOS Pathway in Rats Exposed to Chronic Intermittent Hypoxia. PLoS ONE. 2015; 10:e0131923. [PubMed: 26132492]

8. Žaloudíková M, Vytášek R, Vajnerová O, Hniličková O, Vízek M, Hampl V, Herget J. Depletion of alveolar macrophages attenuates hypoxic pulmonary hypertension but not hypoxia-induced increase in serum concentration of MCP-1. Physiol Res. 2016

9. El Kasmi KC, Pugliese SC, Riddle SR, Poth JM, Anderson AL, Frid MG, Li M, Pullamsetti SS, Savai R, Nagel MA, Fini MA, Graham BB, Tuder RM, Friedman JE, Eltzschig HK, Sokol RJ, Stenmark KR. Adventitial fibroblasts induce a distinct proinflammatory/profibrotic macrophage phenotype in pulmonary hypertension. J Immunol. 2014; 193:597–609. [PubMed: 24928992]

10. Vergadi E, Chang MS, Lee C, Liang OD, Liu X, Fernandez-Gonzalez A, Mitsialis SA, Kourembanas S. Early Macrophage Recruitment and Alternative Activation Are Critical for the Later Development of Hypoxia-Induced Pulmonary Hypertension. Circulation. 2011; 123:1986–1995. [PubMed: 21518986]

11. Maycotte P, Jones KL, Goodall ML, Thorburn J, Thorburn A. Autophagy Supports Breast Cancer Stem Cell Maintenance by Regulating IL6 Secretion. Mol Cancer Res. 2015; 13:651–658. [PubMed: 25573951]

12. Trapnell C, Williams BA, Pertea G, Mortazavi A, Kwan G, van Baren MJ, Salzberg SL, Wold BJ, Pachter L. Transcript assembly and quantification by RNA-Seq reveals unannotated transcripts and isoform switching during cell differentiation. Nat Biotechnol. 2010; 28:511–515. [PubMed: 20436464]

13. Barletta KE, Cagnina RE, Wallace KL, Ramos SI, Mehrad B, Linden J. Leukocyte compartments in the mouse lung: Distinguishing between marginated, interstitial, and alveolar cells in response to injury. Journal of Immunological Methods. 2012; 375:100–110. [PubMed: 21996427]

14. Jakubzick C, Gautier EL, Gibbings SL, Sojka DK, Schlitzer A, Johnson TE, Ivanov S, Duan Q, Bala S, Condon T, Van Rooijen N, Grainger JR, Belkaid Y, Ma'ayan A, Riches DWH, Yokoyama WM, Ginhoux F, Henson PM, Randolph GJ. Minimal Differentiation of Classical Monocytes as They Survey Steady-State Tissues and Transport Antigen to Lymph Nodes. Immunity. 2013; 39:599–610. [PubMed: 24012416]

15. Pugliese SC, Poth JM, Fini MA, Olschewski A, El Kasmi KC, Stenmark KR. The role of inflammation in hypoxic pulmonary hypertension: from cellular mechanisms to clinical phenotypes. Am J Physiol Lung Cell Mol Physiol. 2015; 308:L229–L252. [PubMed: 25416383]

16. Poczobutt JM, De S, Yadav VK, Nguyen TT, Li H, Sippel TR, Weiser-Evans MCM, Nemenoff RA. Expression Profiling of Macrophages Reveals Multiple Populations with Distinct Biological Roles in an Immunocompetent Orthotopic Model of Lung Cancer. J Immunol. 2016; 196:2847–2859. [PubMed: 26873985]

17. Ensan S, Li A, Besla R, Degousee N, Cosme J, Roufaiel M, Shikatani EA, El-Maklizi M, Williams JW, Robins L, Li C, Lewis B, Yun TJ, Lee JS, Wieghofer P, Khattar R, Farrokhi K, Byrne J, Ouzounian M, Zavitz CCJ, Levy GA, Bauer CMT, Libby P, Husain M, Swirski FK, Cheong C, Prinz M, Hilgendorf I, Randolph GJ, Epelman S, Gramolini AO, Cybulsky MI, Rubin BB, Robbins CS. Self-renewing resident arterial macrophages arise from embryonic CX3CR1(+) precursors and circulating monocytes immediately after birth. Nat Immunol. 2016; 17:159–168. [PubMed: 26642357]

18. Madjdpour C, Jewell UR, Kneller S, Ziegler U, Schwendener R, Booy C, Kläusli L, Pasch T, Schimmer RC, Beck-Schimmer B. Decreased alveolar oxygen induces lung inflammation. Am J Physiol Lung Cell Mol Physiol. 2003; 284:L360–L367. [PubMed: 12388372]

19. Chao J, Donham P, Van Rooijen N, Wood JG, Gonzalez NC. Monocyte chemoattractant protein-1 released from alveolar macrophages mediates the systemic inflammation of acute alveolar hypoxia. Am J Respir Cell Mol Biol. 2011; 45:53–61. [PubMed: 20813992]

20. Minamino T, Christou H, Hsieh CM, Liu Y, Dhawan V, Abraham NG, Perrella MA, Mitsialis SA, Kourembanas S. Targeted expression of heme oxygenase-1 prevents the pulmonary inflammatory and vascular responses to hypoxia. Proc Natl Acad Sci USA. 2001; 98:8798–8803. [PubMed: 11447290]

21. Janssen WJ, Barthel L, Muldrow A, Oberley-Deegan RE, Kearns MT, Jakubzick C, Henson PM. Fas Determines Differential Fates of Resident and Recruited Macrophages during Resolution of Acute Lung Injury. Am J Respir Crit Care Med. 2011; 184:547–560. [PubMed: 21471090]

22. Madjdpour C, Jewell UR, Kneller S, Ziegler U, Schwendener R, Booy C, Kläusli L, Pasch T, Schimmer RC, Beck-Schimmer B. Decreased alveolar oxygen induces lung inflammation. Am J Physiol Lung Cell Mol Physiol. 2003; 284:L360–L367. [PubMed: 12388372]

23. van der Meer PF, Gratama JW, van Delden CJ, Laport RF, Levering WH, Schrijver JG, Tiekstra MJ, Keeney M, de Wildt-Eggen J. Comparison of five platforms for enumeration of residual leucocytes in leucoreduced blood components. Br J Haematol. 2001; 115:953–962. [PubMed: 11843833]

24. Gratama JW, Kraan J, Keeney M, Sutherland DR, Granger V, Barnett D. Validation of the single-platform ISHAGE method for CD34(+) hematopoietic stem and progenitor cell enumeration in an international multicenter study. Cytotherapy. 2003; 5:55–65. [PubMed: 12745591]

25. Ginhoux F, Guilliams M. Tissue-Resident Macrophage Ontogeny and Homeostasis. Immunity. 2016; 44:439–449. [PubMed: 26982352]

26. Jin Y, Calvert TJ, Chen B, Chicoine LG, Joshi M, Bauer JA, Liu Y, Nelin LD. Mice deficient in Mkp-1 develop more severe pulmonary hypertension and greater lung protein levels of arginase in response to chronic hypoxia. Am J Physiol Heart Circ Physiol. 2010; 298:H1518–28. [PubMed: 20173047]

27. Smallie T, Ross EA, Ammit AJ, Cunliffe HE, Tang T, Rosner DR, Ridley ML, Buckley CD, Saklatvala J, Dean JL, Clark AR. Dual-Specificity Phosphatase 1 and Tristetraprolin Cooperate To Regulate Macrophage Responses to Lipopolysaccharide. J Immunol. 2015; 195:277–288. [PubMed: 26019272]

28. Zhou H, Liu H, Porvasnik SL, Terada N, Agarwal A, Cheng Y, Visner GA. Heme oxygenase-1 mediates the protective effects of rapamycin in monocrotaline-induced pulmonary hypertension. Lab Invest. 2006; 86:62–71. [PubMed: 16357868]

29. O'Neill LAJ, Hardie DG. Metabolism of inflammation limited by AMPK and pseudo-starvation. Nature. 2013; 493:346–355. [PubMed: 23325217]

30. A-González N, Castrillo A. Liver X receptors as regulators of macrophage inflammatory and metabolic pathways. Biochim Biophys Acta. 2011; 1812:982–994. [PubMed: 21193033]

31. Joseph SB, Castrillo A, Laffitte BA, Mangelsdorf DJ, Tontonoz P. Reciprocal regulation of inflammation and lipid metabolism by liver X receptors. Nat Med. 2003; 9:213–219. [PubMed: 12524534]

32. Beyer C, Huang J, Beer J, Zhang Y, Palumbo-Zerr K, Zerr P, Distler A, Dees C, Maier C, Munoz L, Krönke G, Uderhardt S, Distler O, Jones S, Rose-John S, Oravecz T, Schett G, Distler JHW. Activation of liver X receptors inhibits experimental fibrosis by interfering with interleukin-6 release from macrophages. Ann Rheum Dis. 2015; 74:1317–1324. [PubMed: 24618263]

33. Im SS, Osborne TF. Liver x receptors in atherosclerosis and inflammation. Circulation Research. 2011; 108:996–1001. [PubMed: 21493922]

34. Maron BA, Oldham WM, Chan SY, Vargas SO, Arons E, Zhang YY, Loscalzo J, Leopold JA. Upregulation of steroidogenic acute regulatory protein by hypoxia stimulates aldosterone synthesis in pulmonary artery endothelial cells to promote pulmonary vascular fibrosis. Circulation. 2014; 130:168–179. [PubMed: 25001622]

35. Wang R, Zhou SJ, Zeng DS, Xu R, Fei LM, Zhu QQ, Zhang Y, Sun GY. Plasmid-based short hairpin RNA against connective tissue growth factor attenuated monocrotaline-induced pulmonary vascular remodeling in rats. Gene Ther. 2014; 21:931–937. [PubMed: 25077774]

36. Savale L, Tu L, Rideau D, Izikki M, Maitre B, Adnot S, Eddahibi S. Impact of interleukin-6 on hypoxia-induced pulmonary hypertension and lung inflammation in mice. Respir Res. 2009; 10:6–13. [PubMed: 19173740]

37. Duffield JS, Forbes SJ, Constandinou CM, Clay S, Partolina M, Vuthoori S, Wu S, Lang R, Iredale JP. Selective depletion of macrophages reveals distinct, opposing roles during liver injury and repair. J Clin Invest. 2005; 115:56–65. [PubMed: 15630444]

38. Gibbons MA, MacKinnon AC, Ramachandran P, Dhaliwal K, Duffin R, Phythian-Adams AT, Van Rooijen N, Haslett C, Howie SE, Simpson AJ, Hirani N, Gauldie J, Iredale JP, Sethi T, Forbes SJ. Ly6C hiMonocytes Direct Alternatively Activated Profibrotic Macrophage Regulation of Lung Fibrosis. Am J Respir Crit Care Med. 2011; 184:569–581. [PubMed: 21680953]

39. Nassiri S, Zakeri I, Weingarten MS, Spiller KL. Relative Expression of Proinflammatory and Antiinflammatory Genes Reveals Differences between Healing and Nonhealing Human Chronic Diabetic Foot Ulcers. J Invest Dermatol. 2015; 135:1700–1703. [PubMed: 25647438]
40. Stenmark KR, Meyrick B, Galiè N, Mooi WJ, McMurtry IF. Animal models of pulmonary arterial hypertension: the hope for etiological discovery and pharmacological cure. Am J Physiol Lung Cell Mol Physiol. 2009; 297:L1013–L1032. [PubMed: 19748998]
41. Burke DL, Frid MG, Kunrath CL, Karoor V, Anwar A, Wagner BD, Strassheim D, Stenmark KR. Sustained hypoxia promotes the development of a pulmonary artery-specific chronic inflammatory microenvironment. Am J Physiol Lung Cell Mol Physiol. 2009; 297:L238–L250. [PubMed: 19465514]
42. Wang W, Liu J, Ma A, Miao R, Jin Y, Zhang H, Xu K, Wang C, Wang J. mTORC1 is involved in hypoxia-induced pulmonary hypertension through the activation of Notch3. J Cell Physiol. 2014; 229:2117–2125. [PubMed: 24825564]
43. Houssaini A, Abid S, Mouraret N, Wan F, Rideau D, Saker M, Marcos E, Tissot CM, Dubois-Randé JL, Amsellem V, Adnot S. Rapamycin reverses pulmonary artery smooth muscle cell proliferation in pulmonary hypertension. Am J Respir Cell Mol Biol. 2013; 48:568–577. [PubMed: 23470622]
44. Weichhart T, Hengstschläger M, Linke M. Regulation of innate immune cell function by mTOR. Nature Publishing Group. 2015; 15:599–614.
45. Goncharova EA. mTOR and vascular remodeling in lung diseases: current challenges and therapeutic prospects. FASEB J. 2013; 27:1796–1807. [PubMed: 23355268]
46. Soon E, Holmes AM, Treacy CM, Doughty NJ, Southgate L, Machado RD, Trembath RC, Jennings S, Barker L, Nicklin P, Walker C, Budd DC, Pepke-Zaba J, Morrell NW. Elevated Levels of Inflammatory Cytokines Predict Survival in Idiopathic and Familial Pulmonary Arterial Hypertension. Circulation. 2010; 122:920–927. [PubMed: 20713898]
47. Steiner MK, Syrkina OL, Kolliputi N, Mark EJ, Hales CA, Waxman AB. Interleukin-6 Overexpression Induces Pulmonary Hypertension. Circulation Research. 2009; 104:236–244. [PubMed: 19074475]
48. Parpaleix A, Amsellem V, Houssaini A, Abid S, Breau M, Marcos E, Sawaki D, Delcroix M, Quarck R, Maillard A, Couillin I, Ryffel B, Adnot S. Role of interleukin-1 receptor 1/MyD88 signalling in the development and progression of pulmonary hypertension. Eur Respir J. 2016; 48:470–483. [PubMed: 27418552]
49. Semenza GL. Hypoxia-Inducible Factors in Physiology and Medicine. Cell. 2012; 148:399–408. [PubMed: 22304911]
50. George PM, Oliver E, Dorfmuller P, Dubois OD, Reed DM, Kirkby NS, Mohamed NA, Perros F, Antigny F, Fadel E, Schreiber BE, Holmes AM, Southwood M, Hagan G, Wort SJ, Bartlett N, Morrell NW, Coghlan JG, Humbert M, Zhao L, Mitchell JA. Evidence for the involvement of type I interferon in pulmonary arterial hypertension. Circulation Research. 2014; 114:677–688. [PubMed: 24334027]
51. Pendergrass SA, Hayes E, Farina G, Lemaire R, Farber HW, Whitfield ML, Lafyatis R. Limited Systemic Sclerosis Patients with Pulmonary Arterial Hypertension Show Biomarkers of Inflammation and Vascular Injury. PLoS ONE. 2010; 5:e12106–13. [PubMed: 20808962]
52. Christmann RB, Hayes E, Pendergrass S, Padilla C, Farina G, Affandi AJ, Whitfield ML, Farber HW, Lafyatis R. Interferon and alternative activation of monocyte/macrophages in systemic sclerosis-associated pulmonary arterial hypertension. Arthritis & Rheumatism. 2011; 63:1718–1728. [PubMed: 21425123]
53. Paulin R, Courboulin A, Meloche J, Mainguy V, Dumas de la Roque E, Saksouk N, Cote J, Provencher S, Sussman MA, Bonnet S. Signal Transducers and Activators of Transcription-3/Pim1 Axis Plays a Critical Role in the Pathogenesis of Human Pulmonary Arterial Hypertension. Circulation. 2011; 123:1205–1215. [PubMed: 21382889]
54. Johns RA, Takimoto E, Meuchel LW, Elsaigh E, Zhang A, Heller NM, Semenza GL, Yamaji-Kegan K. Hypoxia-Inducible Factor 1α Is a Critical Downstream Mediator for Hypoxia-Induced Mitogenic Factor (FIZZ1/RELMα)-Induced Pulmonary Hypertension. Arteriosclerosis, Thrombosis, and Vascular Biology. 2016; 36:134–144.

55. Goncharov DA, Kudryashova TV, Ziai H, Ihida-Stansbury K, DeLisser H, Krymskaya VP, Tuder RM, Kawut SM, Goncharova EA. Mammalian target of rapamycin complex 2 (mTORC2) coordinates pulmonary artery smooth muscle cell metabolism, proliferation, and survival in pulmonary arterial hypertension. Circulation. 2014; 129:864–874. [PubMed: 24270265]

56. Aghamohammadzadeh R, Zhang YY, Stephens TE, Arons E, Zaman P, Polach KJ, Matar M, Yung LM, Yu PB, Bowman FP, Opotowsky AR, Waxman AB, Loscalzo J, Leopold JA, Maron BA. Up-regulation of the mammalian target of rapamycin complex 1 subunit Raptor by aldosterone induces abnormal pulmonary artery smooth muscle cell survival patterns to promote pulmonary arterial hypertension. FASEB J. 2016; 30:2511–2527. [PubMed: 27006450]

57. Byles V, Covarrubias AJ, Ben-Sahra I, Lamming DW, Sabatini DM, Manning BD, Horng T. The TSC-mTOR pathway regulates macrophage polarization. Nat Commun. 2013; 4:2834. [PubMed: 24280772]

58. Moon JS, Hisata S, Park MA, DeNicola GM, Ryter SW, Nakahira K, Choi AMK. mTORC1-Induced HK1-Dependent Glycolysis Regulates NLRP3 Inflammasome Activation. Cell Reports. 2015; 12:102–115. [PubMed: 26119735]

59. Ginhoux F, Schultze JL, Murray PJ, Ochando J, Biswas SK. New insights into the multidimensional concept of macrophage ontogeny, activation and function. Nat Immunol. 2016; 17:34–40. [PubMed: 26681460]

60. Hume DA. Applications of myeloid-specific promoters in transgenic mice support in vivo imaging and functional genomics but do not support the concept of distinct macrophage and dendritic cell lineages or roles in immunity. Journal of Leukocyte Biology. 2011; 89:525–538. [PubMed: 21169519]

61. Gheryani N, Coffelt SB, Gartland A, Rumney RMH, Kiss-Toth E, Lewis CE, Tozer GM, Greaves DR, Dear TN, Miller G. Generation of a novel mouse model for the inducible depletion of macrophages in vivo. Genesis. 2013; 51:41–49. [PubMed: 22927121]

62. McCubbrey AL, Barthel L, Mould KJ, Mohning MP, Redente EF, Janssen WJ. Selective and inducible targeting of CD11b+ mononuclear phagocytes in the murine lung with hCD68-rtTA transgenic systems. Am J Physiol Lung Cell Mol Physiol. 2016; 311:L87–L100. [PubMed: 27190063]

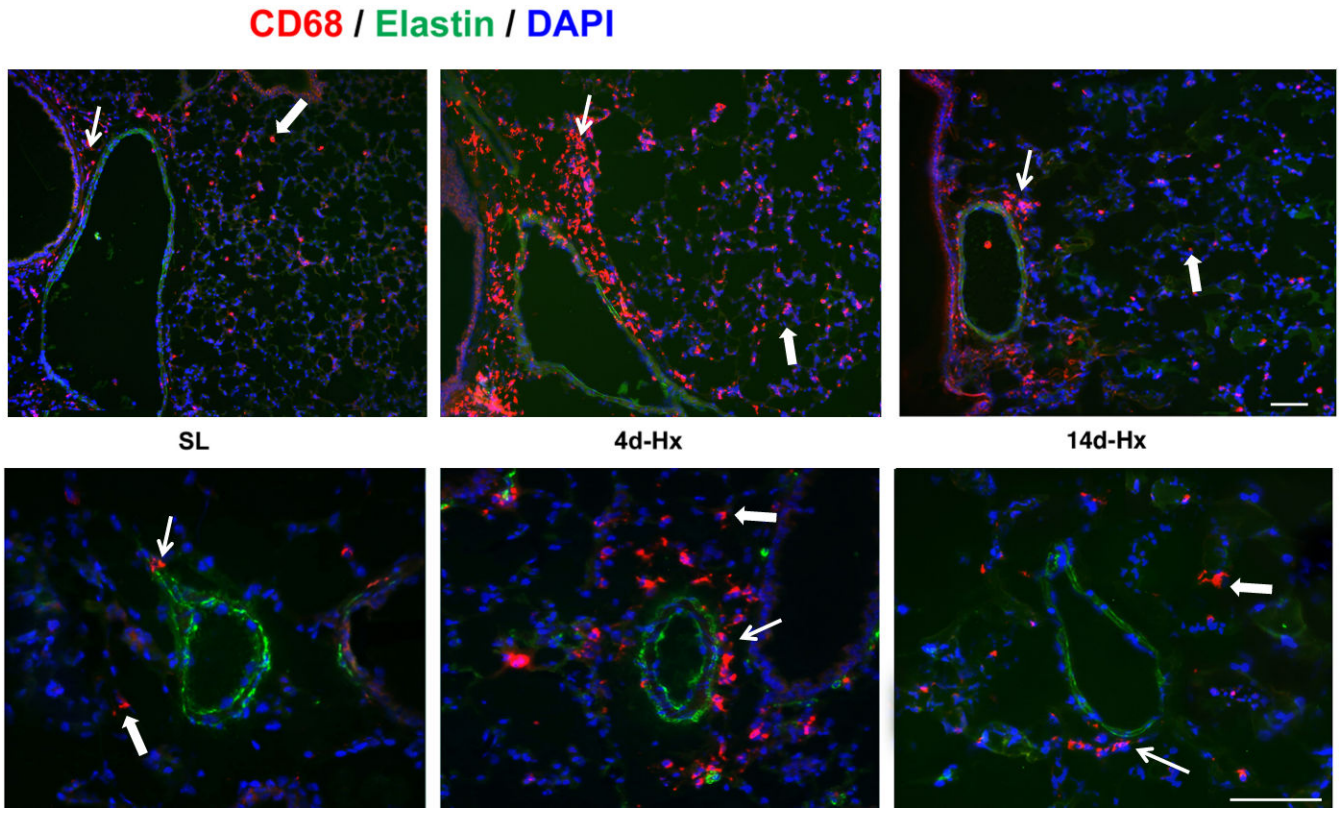

Figure 1.

Accumulation of CD68-positive perivascular macrophages (red) is observed at 4 days and 14 days hypoxic (simulated 18,000 feet) exposure in WT mice, compared to sea-level controls. Thin arrows label perivascular macrophages while thick arrows label alveolar macrophages. Cell nuclei are labeled with DAPI (blue), elastic lamellae (green) are visualized via autofluorescence. Scale bar 100 μm. SL, sea level; 4d-Hx, 4 days hypoxia; 14d-Hx, 14 days hypoxia. Representative of 5 mice per group.

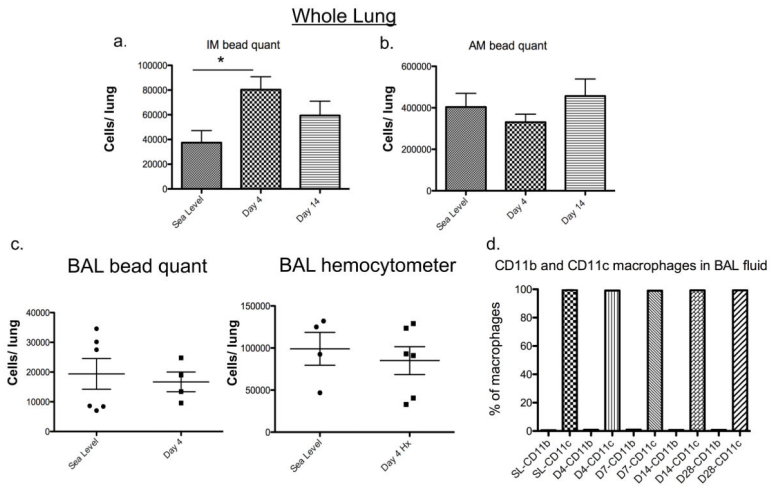

Figure 2.

FACS quantification of lung macrophages. **a,b** WT mice were exposed to hypoxia for 4, 14 days or remained at sea level. IM's and AM's were quantified using whole lung via flow cytometry. IM's and AM's expressed as total number per lung determined by FACS/ counting bead method. N= 5 mice per group. Error bars show SEM. * $p<0.05$. **c:** Cells were lavaged from sea level mice or after 4 days of hypoxia exposure. Macrophages were quantified using counting beads and FACS or by hemocytometer. N=4–6 mice per group. There were no significant differences between groups. **d**. Time course of CD64+, $CD11b^{hi}$ or CD64+, $CD11c^{hi}$ cells represented as percentage of macrophages in BAL fluid. No significant differences between groups. N=4–5 mice per group. Quant, quantification; BAL, bronchoalveolar lavage; SL, sea level; D, day; WT, wild type; IM, interstitial macrophage; AM, alveolar macrophage.

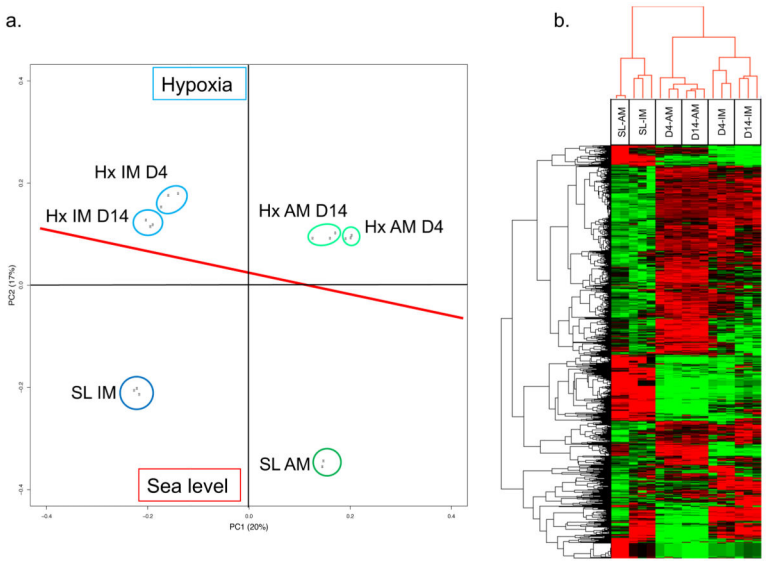

Figure 3.

a. Principle component analysis (PCA) of AM's and IM's at baseline and after 4 and 14 days hypoxia exposure. Each dot represents RNAseq data from 3 pooled mice performed in biologic triplicate except for sea level AM's which were done in biologic replicate. Power analysis demonstrated 99% power for sample size with a p value<0.05. The red line separates sea level samples from hypoxic samples. **b.** Global analysis of differentially expressed genes between AM and IM populations. Identification of differentially expressed genes was performed in all pairwise comparisons between the cell population (AMs & IMs) and between different time points (0, 4 & 14 day hypoxia) from the RNA-seq analysis (2,672 genes). Hierarchical clustering and heatmap were generated on the set of 2,672 genes and highly expressed genes in specific populations were clustered. Cluster of RNA-seq data segregated in two clusters (sea level and hypoxia) and further segregated in AMs and IMs. SL, sea level; IM, interstitial macrophage; AM, alveolar macrophage; D, day.

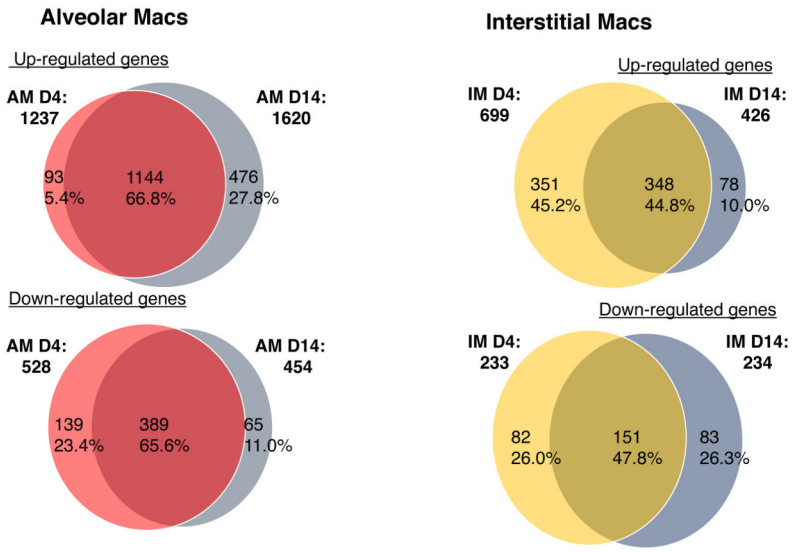

Figure 4.

VENN diagrams showing up and down regulated genes in alveolar macrophages (AM) and interstitial macrophages (IM) after 4 days (D4) or 14 days (D14) hypoxia as compared to baseline sea level macrophages. Listed are total numbers of differentially regulated genes in each subset as well as the percentages of total up or down regulated genes in each group. Cutoff criteria for differential gene expression: ≥ 2 fold absolute change from sea level baseline, $q<0.05$.

Figure 5.

IPA analysis of top canonical pathways and upstream regulators in alveolar and interstitial macrophages. **a.** List of all canonical pathways and **b.** upstream regulators (abbreviated list) with a $p<0.05$, absolute $Z \geq 2$ in AM's and IM's after 4 or 14 days hypoxia as compared to baseline sea level macrophages. Colors indicate higher or lower Z scores. **c.** List of top canonical pathways (abbreviated list) in IM's and AM's after 4 or 14 days hypoxia with a $p<0.05$ sorted by increasing p values (dark purple color). IM, interstitial macrophage; AM, alveolar macrophage; D, day.

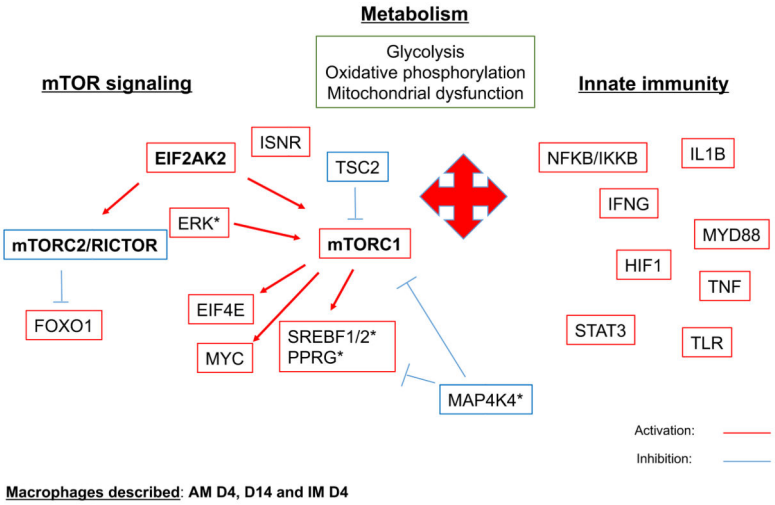

Figure 6.

Schematic of the major pathways/upstream regulators and their interaction as identified by IPA analysis in AM's at days 4 and 14 and IM's at day 4. Red boxes indicate predicted activation, while blue boxes predicted inhibition with an absolute Z score cutoff of 2 and a $p<0.05$. Red arrows indicate activation of downstream pathway, while blue lines indicate inhibition of downstream pathway. * ERK was not significant in AM's at days 4 or 14, while MAP4K4, PPRG, SREBF1/2 were not significant in IM's at day 4.

Figure 7 a:

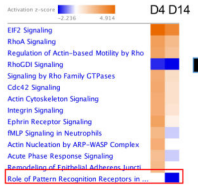

Unique Canonical pathways IM D14

Canonical pathway	Z score, P value	Genes
Role of pattern recognition receptors in bacteria and viruses	**IM D14**: -2.236, 0.04 IM D4: NS	↓: FGFR1, IL6, IRF7, MAPK3, OAS3, PRKCB

Figure 7 b:

Unique upstream regulators IM D14

Upstream regulator	IM D14 Z score	IM D4 Z score	Function
NR1H3	2.19	NS	Liver x receptor: cholesterol metabolism, anti-inflammatory in macrophages
NR1H2	2.19	NS	liver x receptor
NR1H	2.19	NS	liver x receptor
DUSP1	2.17	-0.94	anti-inflammatory
HMOX1	2.17	NS	anti-inflammatory
WT1	2.15	NS	anti-inflammatory via IL-10 activation
STK11	2.00	NS	tumor suppressor gene
Irgm1	2.00	NS	interferon signaling
TGM2	-2.55	NS	apoptosis, marker of macrophage polarization
MYD88	-2.47	1.50	TLR4 signaling
CCL5	-2.41	1.91	CCR5 ligand, promotes macrophage recruitment and survival
PDGF-BB	-2.23	0.16	growth factor
ERK 1/2	-2.23	-0.04	MAP kinase signaling
TLR 2	-2.23	NS	innate immune signaling
PTGS2	-2.21	NS	prostacyclin synthase-makes prostacyclin
ITGB1	-2.20	NS	integrin, cell adhesion
IRF3	-2.19	NS	interferon signaling
PTGER2	-2.11	1.40	prostaglandin signaling
TLR 9	-2.00	NS	innate immune signaling

Figure legends: *z score > |2|, P ≤ 0.05)

Figure 7.

a. Canonical pathways in IM's after 4 and 14 days hypoxic exposure as compared to baseline sea level macrophages. "Role of pattern recognition receptors in bacteria and viruses" was the only pathway with an absolute Z score>2, p<0.05 that was unique in IM's at day 14 as compared to IM's at day 4. The individual genes in this pathways are listed with the down arrow indicating decreased transcription as compared to baseline sea level macrophages. **b**. Selected unique upstream regulators in IM's after 14 days hypoxia with an absolute Z score>2, p<0.05. Table denotes Z score of corresponding regulator in IM's after 4 days hypoxia. IM, interstitial macrophage; AM, alveolar macrophage; D, day; NS, non-significant.

Programming changes D4 compared to D14 IM

Top Canonical pathways	Z score	Adjusted p value
Acute phase response signaling	-2.00	9.31E-06
Fcγ Receptor-mediate phagocytosis in macrophages and monocytes	-3.87	1.33E-04
Integrin signaling	-2.13	1.48E-04
Leukocyte extravasation signaling	-2.18	2.17E-04

Upstream regulators

Activated	Function
IL10RA	anti-inflammatory
ACKR2	inhibits th17 response
DUSP1	anti-inflammatory
Nr1h	Liver x receptor- anti-inflammatory, macrophage polarization
JAG2	notch ligand, pro-angiogenesis, anti-inflammatory, pro-EMT
CTGF	pro-remodeling, implicated in PH and fibrosis
TSC2	Decreased MTORC1
IL1RA	Inhibits IL1 signaling
ZPF36	inhibits NFKb activity, TNF
SOCS1	Inhibits STAT1 signaling
ENG	Endoglin- TGFB signaling

Inhibited pathways	Function
IRF7, IRF3, IRF1, IRF5	Interferon signaling
TLR3, TLR9, TLR4, TLR7, TLR2	Innate immune signaling
TNF	Innate immune signaling
EIF2-AKT2	Protein synthesis
IFNA2, IFNG,	Interferon signaling
STAT1	Interferon signaling
NFKB	Innate immune signaling
EIF4E	Protein translation
MYD88	Innate immune signaling

Figure 8.

All canonical pathways and upstream regulators in IM's after 14 days of hypoxia as compared to IM's after 4 days hypoxia with an absolute Z score≥ 2, $p<0.05$. Adjusted p value (q value) is listed in the table for canonical pathways. The filtered data set used for IPA used the cutoff of $q<0.2$ and an absolute fold change of ≥1.5.